Pergamon

Tetrahedron 55 (1999) 14915–14924

TETRAHEDRON

Ab Initio Molecular Orbital Study on Three Feasible Mechanisms for Substitution of the Vinylic Carbon in $F_2C=C(OMs)BMe_3^-$.

Kenzi Hori,[#,*] Shohei Fukuda,[#] Junji Ichikawa[&]

[#]Department of Applied Chemistry, Faculty of Engineering, Yamaguchi University, Ube 755-8611, Japan,
[&] Department of Chemistry, Graduate School of Science, The University of Tokyo, Hongo, Tokyo, 113-0033, Japan

Received 21 June 1999; accepted 29 October 1999

Abstract: A substitution on 2,2-difluorovinylic carbon was investigated by using *ab initio* molecular orbital calculations. Three feasible mechanisms, which are the S_N1-like, the S_N2-type and the addition-elimination mechanisms, were examined for a model borate, 2,2-difluoro-1-mesyloxyvinyl(trimethyl)borate. Four TSs were obtained depending on the position of Li^+ around the vinylborate although activation energies in the gas phase are rather high (ca. 30–40 kcal mol^{-1}) in comparison with that expected from the experimental conditions. It was confirmed at the SCRF-IPCM calculations that the solvent effect reduces the activation energy of one S_N2-type mechanism very much (4.1 kcal mol^{-1} at the B3LYP/6-31+G*//RHF/6-31+G* level of theory) while those for the other mechanisms do not change very much. Therefore, the S_N2-type mechanism is applicable to the substitution reaction observed for the vinylborate.

INTRODUCTION

Nucleophilic vinylic substitutions have been a subject of considerably strong interest in both synthetic and mechanistic studies. Among them, substitution on 2,2-difluorovinylic carbon was achieved in the reaction of 2,2-difluorovinyl anion **2a** with trialkylboranes through borate complexes **3a** shown in Eq. 1.[1] The 1,2-migration of an alkyl group from the boron to the vinylic carbon bearing tosyloxy group generates

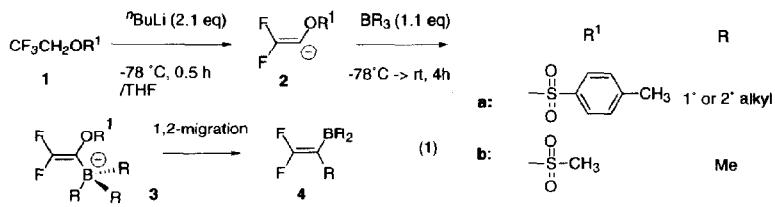

*To whome corresponding should be addressed. E-mail:kenji@sparklx.chem.yamaguchi-u.ac.jp

0040-4020/99/$ - see front matter
PII: S0040-4020(99)00976-X

difluorovinylboranes **4a**, which are powerful intermediates for synthesis of gem-difluoro compounds.[2] This sequence includes a quite unique substitution on 2,2-difluorovinylic position. This position is deactivated toward nucleophilic attack by the two fluorine substituents while the terminal difluoromethylene carbon is highly activated.[3]

It is possible to consider three paths of the mechanisms from **3** to **4** shown in Scheme 1. The first is an S_N1-like mechanism: R^1O^- first leaves to form an intermediate like vinylic cation, followed by migration of R on the boron to the vinylic carbon. This mechanism may cause mixing of configurations around the vinylic carbon and such a reaction has not been observed yet. In our previous paper,[4] we discussed possibility of this mechanism using results of *ab initio* molecular orbital (MO) calculations at the MP2/6-31+G*//RHF/6-31+G* level of theory. It was confirmed that the route had a rather high activation energy in comparison with that expected from the experimental conditions.

Scheme 1

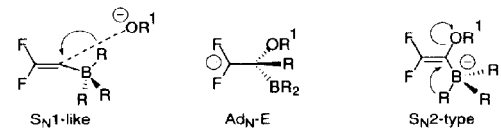

As ordinal substitutions on vinylic carbons are thought to proceed through addition–elimination (Ad_N–E) mechanism,[5] the reaction in Eq. 1 may take place *via* an intermediate with a rather unstable CF_2^- fragment, the second route. The last is an S_N2-type mechanism, where one of the Rs in the BR_3 fragment nucleophilically attacks the vinylic carbon with the OR^1 group (OTs in the experiments). This mechanism accompanies inversion of configuration around the vinylic carbon as observed in fluorine-free systems.[6] Both experimental[6,7] and theoretical investigations[8] demonstrated possibility of this unique mechanism. Although the similar system[6] was confirmed to proceed through the S_N2-type mechanism, it is impossible to prove which mechanism is applicable to the reaction of Eq. 1 because all the mechanisms produce the same product as **3a** has the CF_2 fragment.

Scheme 1 includes no counter cation Li^+. The cation can stabilize the unstable CF_2 fragment in the Ad_N–E intermediate. In fact, we could not obtain any stable geometries without the counter ion for the intermediate of this mechanism as will be discussed later. The interaction between the cation and the negatively charged atoms in **3** results in change of the energy relation among related intermediates and TSs. Midland pointed out that Lewis acid is effective to reduce the barrier height in a saturated borate system.[9] Our experiments used polar solvent such as THF, which largely relates to stability of the intermediates considered in the present study as well. It is likely that the effects of the cation and solvents largely affect the mechanisms which are applicable to the reaction of Eq. 1.

In the present study, our attention was focused on the possibility of the S_N2-type and the Ad_N–E mechanisms. Several geometries of model compounds having a Li^+ ion were considered in order to include the effect of the counter cation in *ab initio* molecular orbital (MO) calculations at the B3LYP/6-31+G*//RHF/6-31+G* and MP2/6-31+G**//RHF/6-31+G* level of theory. We also investigated how the solvent effect relates to the height of the activation energies for each mechanism. The SCRF energies at the RHF/6-31+G* level of theory were calculated for optimized intermediates and TSs in order to qualitatively estimate the solvent effect. The calculations using the model molecules indicated that the reaction in Eq. 1 proceeded through the S_N2-type mechanism.

Table 1. Energies[1] for intermediates and TSs related to the substitution on vinylic carbon.

Molecule	E(RHF)	E(B3LYP)	E(SCRF)[2]	E(MP2)	ΔE(RHF)	ΔE(B3LYP)	ΔE(MP2)	ΔE(Solv)[2]
5b	-1087.23366	-1091.75339	-1087.27205	-1089.26701	16.8	15.5	16.0	13.9(14.1)
6b	-1087.26044	-1091.77806	-1087.28581	-1089.29255	0.0	0.0	0.0	6.6(6.3)
7b	-1087.23287	-1091.74837	-1087.29843	-1089.26234	17.3	18.6	19.0	0.0(0.0)
8b	-1087.27279	-1091.77641	-1087.30116	-1089.28826	-7.8	1.0	2.7	5.7(7.1)
TS(S_N2Li-1)	-1087.19144	-1091.71538	-1087.23541	-1089.21348	43.3	39.3	49.6	34.3(44.2)
TS(S_N2Li-2)	-1087.20411	-1091.72945	-1087.28213	-1089.23771	35.3	30.5	34.4	4.1(7.6)
TS(Ad_N-E)	-1087.17914	-1091.71010	-1087.20152	-1089.21460	51.0	42.6	48.9	51.1(57.0)
TS(S_N1Li)	-1087.19796	-1091.71482	-1087.22034	-1089.20488	39.2	39.7	55.0	48.1(63.2)

[1] E(X) are total energies in Hartree unit and ΔE(X) are energies relative to the most stable intermediates in kcal mol^{-1} unit.

[2] See Ref. 15. Values are energies relative to that of **7b** at the MP2/6-31+G**//RHF/6-31+G* (MP2/6-31+G**//RHF/6-31+G*) level of theory.

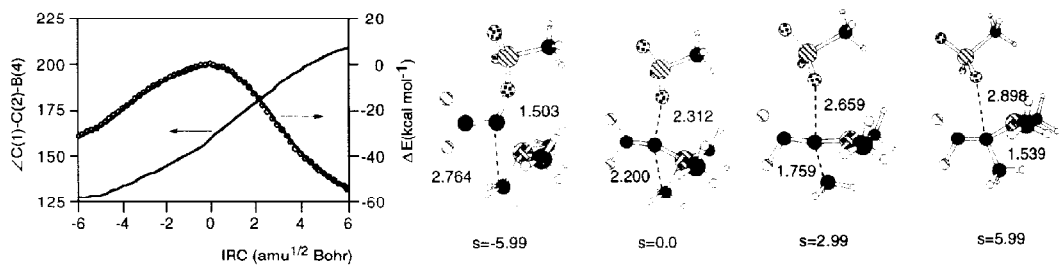

Figure 1 Geometry Transformation along the IRC for the S_N2-type Mechanism without Li^+.

METHOD OF CALCULATIONS

The model anion for the present study is **3b** which possesses three methyl and mesyl groups instead of three primary or secondary alkyl and tosyl groups. We used the Gaussian 94 program[10] on the NEC HSP computer at the computer center, Institute for Molecular Science and workstations of our laboratory. The 6-31+G* basis sets were served to optimize stable and TS structures. The vibration frequency calculation showed that the TS structures have only one imaginary frequency. The intrinsic reaction coordinates (IRCs)[11] were calculated to analyze the mechanism in detail at the RHF/6-31+G* level of theory.

In order to estimate the correlation effect on activation energies at the B3LYP/6-31+G*//RHF/6-31+G* and MP2/6-31+G**//RHF/6-31+G* level of theory[12], ΔE(B3LYP) and ΔE(MP2), were calculated for the optimized structures.[13] The SCRF energies of the IPCM model at the RHF/6-31+G* level of theory, E(SCRF), were calculated in order to take solvent effect into account.[14] It is because the model molecules were still too big to calculate the B3LYP or MP2 energies including the effect. We used Eq. 2 in order to calculate energy E(solv) having both the effects,

$$E(solv) = E(X) + (E(SCRF) - E(RHF)) \quad (X= B3LYP \text{ or } MP2) \qquad (2),$$

where E(RHF) is the total energy of a optimized geometry at the RHF/6-31+G* level of theory. The energy differences in solution ΔE(solv) were calculatioed by using the E(solv). Table 1 lists all the energies related to the substitution on the vinylic carbon.[15]

RESULTS AND DISCUSSIONS

S_N2-type Mechanism without Li^+.

Before considering substitution mechanisms with the counter cation, an S_N2-type mechanism without Li^+ are investigated. This mechanism, in which CH_3 and MsO fragments in **3b** are a nucleophile and a leaving group, accompanies inversion of stereochemistry around the vinylic carbon. The results of theoretical calculations shown in Figure 1 clearly show this important change in geometry of the mechanism. The ∠C(1)-C(2)-B(4) angle in the geometry at s= -5.99 $amu^{1/2}$ Bohr is 128.0° and increases monotonically up to s= 5.99 $amu^{1/2}$ Bohr, where this angle is 209.6°. The product with a inverted boryl fragment was observed by Brown *et al.* by using a similar system without fluorine substituents.[6] The activation energy of this S_N2-type mechanism was calculated to be 30.8 (39.1) kcal mol^{-1} at the B3LYP/6-31+G*//RHF/6-31+G* (MP2/6-31+G**//RHF/6-31+G*) level of theory. Although we used the model molecules, this barrier is considered to be higher than that expected from our experimental conditions: the reactions proceed at room temperature.

Stable Geometries of 3b Interacting with Li^+.

There are three positions where the Li^+ can locate stably around the anionic intermediate **3b** shown in Figure 2 since it has three types of negatively charged atoms, i.e., F, B and O atoms in CF_2, $B(CH_3)_3$ and mesyl fragments. In the first intermediate **5b**, the Li^+ interacts with both F(9) and B(4). The second intermediate **6b** has the cation bridging B(4) and O(11) in the mesyl fragment. The electrostatic interaction between the Li^+ and F(8) as well as O(10) contributes to forming the third intermediate **7b**. At the B3LYP/6-31+G*//RHF/6-31+G* (MP2/6-31+G**//RHF/6-31+G*) level of theory, the energies relative to **6b** in Table

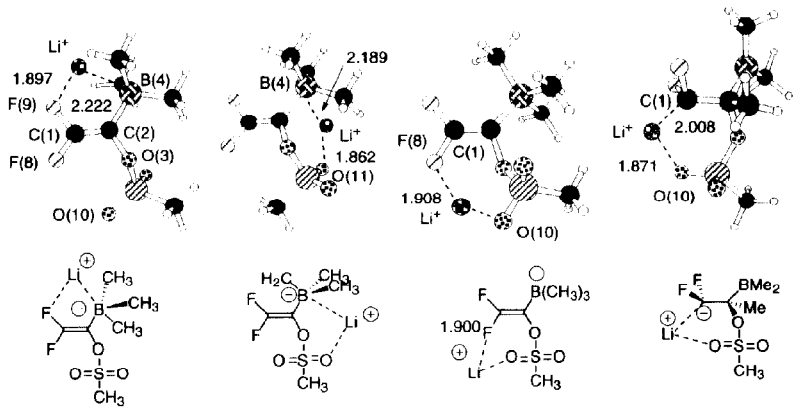

5b **6b** **7b** **8b**

Figure 2 Optimized Geometries of intermediates with a Li^+ ion of the counter cation.

l are 15.5(16.0) and 18.6(19.0) kcal mol^{-1} for **5b** and **7b**, i.e., these intermediates are stable in the order, **6b** > **5b** > **7b**. As will be discussed later, we found four TSs depending on the Li^+ position; **6b** is the reactant for an S_N1-like and for one S_N2-type mechanism; **7b** for the other S_N2-type and an Ad_N–E mechanism. It is necessary to emphasize that two TSs for the S_N2-type mechanism were obtained. On the other hand, **5b** was confirmed not to relate to the present substitution reactions.

Addition-Elimination Mechanism.

The Ad_N–E mechanism, in which anion attacks the vinylic carbon with a leaving group to form an anionic intermediate, is the most common route for the substitution reaction of the vinylic position. In the present case, a methyl group in the $B(CH_3)_3$ fragment acts as a nucleophile and attacks the C(2) to form an anionic intermediate. However, no stable geometry was obtained for such an intermediate without Li^+. It is not so difficult to expect this result since the migration of the methyl group results in forming the intermediate with a very unstable CF_2^- fragment. On the other hand, the optimization including a Li^+ gave a stable geometry of the intermediate **8b** as shown in Figure 2. The terminal CF_2 carbon of the intermediate takes sp^3 hybridization making a lone pair orbital. This orbital can interact with the Li^+ to reduce instability of the CF_2^- fragment so that the Ad_N–E intermediate can exist. The Li-C(1) was calculated to be 2.008 Å in length.

It is necessary to find a TS geometry for the Ad_N–E mechanism in order to confirm that there exists a path connecting **8b** and **3b** with Li^+. A TS with the tetrahedrally distorted CF_2^- fragment was obtained as shown in Figure 3 (s=0.0 $amu^{1/2}$ Bohr) together with several geometries along the IRC. In the geometry at s= 5.99 $amu^{1/2}$ Bohr, the C(1) of the CF_2 fragment takes sp^3 hybridization and interacts with the Li^+ like that in **8b**. Although the C(2)-B(4)-C(5) is 86.0° in angle at the TS, the C(2) is still apart by 2.270 Å from the C(5). The $C(5)H_3$ group locates over the CCF_2 plane in the geometry of s= –2.99 $amu^{1/2}$ Bohr. As the Li^+ in the geometry of s= –5.99 occupies the position between the O(10) of the mesyl group and F(8), this geometry resembles to **7b**. Therefore, the obtained TS connects **8b** and **7b**.

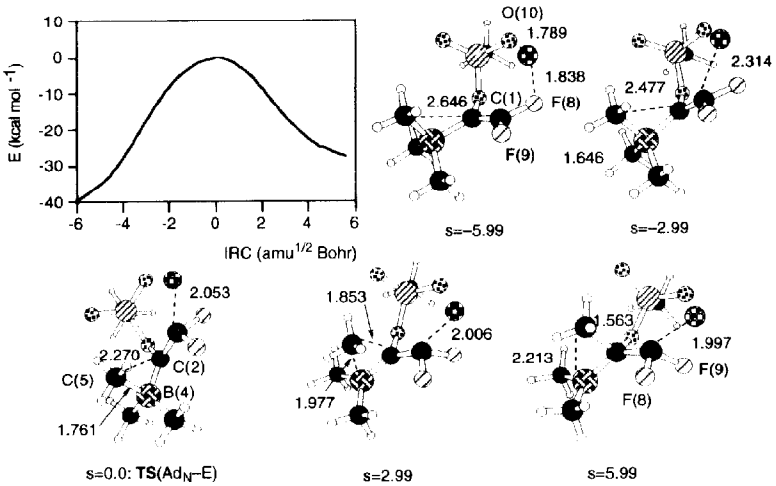

Figure 3 Potentail energy and geometry transformation along the IRC of the Ad_N–E mechanism.

S_N1–like S_N2-Type Mechanisms with Li$^+$.

Although S_N1-like and S_N2-type mechanisms are not as common as the Ad_N–E mechanism for substitution mechanism on vinylic carbon, we also obtained corresponding TS structures shown in Figure 4. In our previous paper,[4] we reported that the C(2)-O(3) length (3.800 Å) in **TS**(S_N1Li) is much longer than that in the similar TS without Li$^+$. **TS**(S_N1Li) has an almost linear C(1)-C(2)-B(4) fragment (176.2°) like a vinyl cation. While C(6) and C(7) locates over and under the CF_2C plane, C(5) locates in the plane. This geometry is suitable for migrating the methyl group through the S_N1-like mechanism with the retention of configuration. The position of the Li$^+$ indicates that the TS comes from **6b**.

The Li$^+$ occupies the position between O(3) and B(4) in **TS** (S_N2Li-1). The IRC calculation also confirmed that the reactant **6b** is connected with the TS. While the C(2)-O(3) in the TS is longer in length by almost 0.5 Å than that in **6b**, the changes in lengths of Li- O(3) and Li-B(4) are rather small, less than 0.121 Å. The latter change in geometry is convenient to getting electrostatic interactions among these atoms and stabilizing the TS during the substitution.

The position of Li$^+$ in the **TS**(S_N2Li-2), which has the Li-O(10) of 1.874 Å and Li-F(8) of 2.032 Å, resembles to that in **7b**. This position is also convenient to getting electrostatic stabilization between Li$^+$ and F(8) as well as O(10). The C(2)-O(3) of **TS**(S_N2Li-2) is shorter by 0.248 Å in length than that of **TS**(S_N2Li-1) while the C(2)-C(6) distances differ only by 0.006 Å.

Figure 5 represents the result of the IRC calculation using **TS**(S_N2Li-2). The geometry at s=–4.28 amu$^{1/2}$ Bohr is similar to that of **7b**. In the geometry at s=- 1.98 amu$^{1/2}$ Bohr, the C(2)-O(3) is 1.759 Å so that this bond has already broken. Although the MsO^- group locates far from C(2) in **3b**, i.e., the C(2)-O(3)=2.871 Å at s= 7.99 amu$^{1/2}$ Bohr, the C(1)-C(2)-B(4) fragment does not take a typical sp^2 structure yet since the angle is still 149.0°. The Li$^+$ occupies the position between F(8) and O(10) and the electrostatic

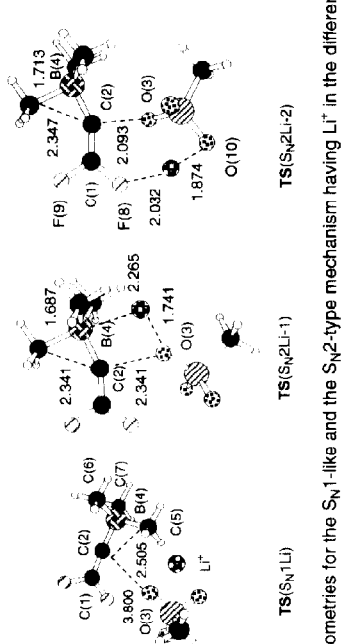

Figure 4. TS geometries for the S_N1-like and the S_N2-type mechanism having Li^+ in the different position around **3b**.

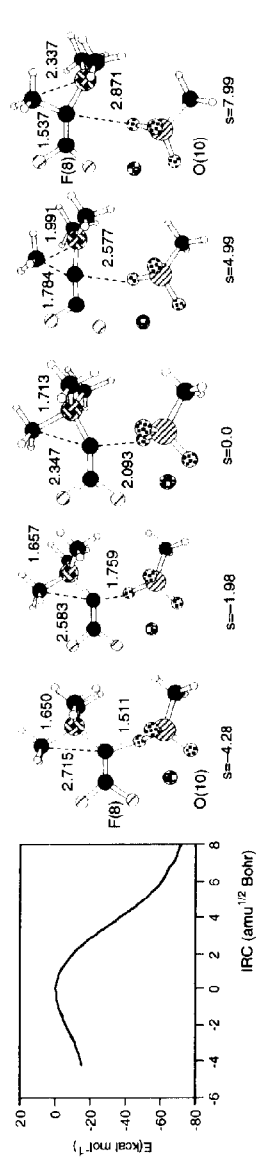

Figure 5. Potentail energy and geometry transformation along the IRC of the S_N2-type mechanism via **TS**(S_N2Li-2).

interaction assists that **3b** releases the mesyloxy group. This figure clearly shows that a methyl group makes a new C(2)-C(5) bond at the opposite side of the leaving mesyloxy group.

Activation Energies of Each Mechanism.

It is quite important to note again here that there exist four TSs depending on the position of the counter cation; two of them are TSs for the S_N2-type mechanism, one for the Ad_N–E and one for the S_N1-like mechanism. In order to determine which is the most favorable route for the substitution mechanism, it is necessary to estimate activation energies for the corresponding TSs.

In the gas phase, the activation energy for the S_N1-like mechanism, the energy difference between **6b** and **TS**(S_N1Li), was calculated to be 39.7(55.0) kcal mol^{-1} at the B3LYP/6-31+G*//RHF/6-31+G* (MP2/6-31+G**/RHF/6-31+G*) level of theory (ΔE(B3LYP) or ΔE(MP2) in Table 1). The energy difference between **6b** and **TS**(S_N2Li-1), the activation barrier for the first S_N2 route, turned out to be 39.3(49.6) kcal mol^{-1}. On the other hand, the second S_N2 route through **TS**(S_N2Li-2) has a barrier of 11.9(15.4) kcal mol^{-1} because the IRC calculations confirmed the TS to be connected with **7b**. However, **6b** is more stable by 18.6(19.0) kcal mol^{-1} than **7b**, which should not be the reactant used for calculating the activation energy of the second S_N2-type mechanism. The activation energy from **6b** turned out to be 30.5(34.4) kcal mol^{-1}. A similar discussion is applicable to the barrier height for the Ad_N–E mechanism since the IRC calculation using **TS**(Ad_N–E) produces **7b** as the reactant. The activation energy of the Ad_N–E mechanism was calculated to be 42.6(48.9) kcal mol^{-1}. Although the value for the second S_N2-type mechanism is the smallest in the four activation energies in the gas phase, all the energies are larger than that expected from the experimental results; the reaction proceeds at room temperature.

The counter ion Li^+ is surrounded by THF in the experimental conditions of Eq. 1. As the polar solvents strongly interact with Li^+, solvent effect should be included in calculating the activation energies. In order to estimate the solvent effect for the energies, the SCRF calculations of the IPCM method at the

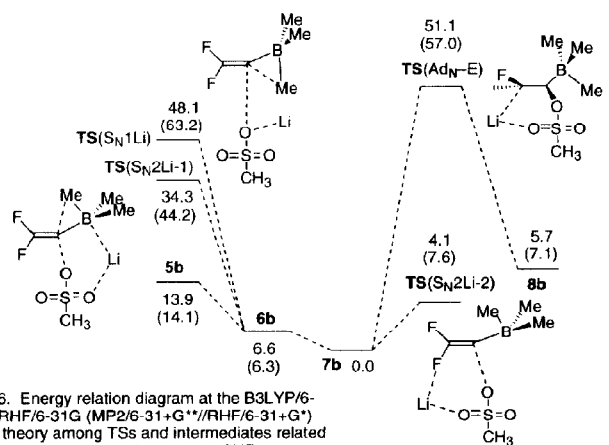

Figure 6. Energy relation diagram at the B3LYP/6-31+G*/RHF/6-31G (MP2/6-31+G**//RHF/6-31+G*) level of theory among TSs and intermediates related to substitution on the vinylic carbon in THF.

RHF/6-31+G* level of theory were carried out in a dielectric of THF.[14b] Figure 6 displays the energy relation diagram in THF by using the energies discussed above in Eq. 2.

The solvation energies for the intermediates and TSs are highly dependent on how easy Li^+ can interact with solvents. While the Li^+ in **7b** interacts with F(8) and O(10), no other substituents disturbe the interaction between Li^+ and solvents. On the other hand, the cation interacts with the B(4)Me_3 fragment of **5b** and **6b**, in which the two methyl groups prevent the cation from interacting with solvents. As the results, the order of the stability of the intermediates in THF is different from that in the gas phase. It was calculated that **7b** is the most stable in THF and is more stable than **6b** and **5b** by 6.6(6.3) and 13.9(14.1) kcal mol^{-1}. Therefore, **7b** is the reactant in THF. The feature of the geometry in **TS**(S_N2Li-2) is enhanced and stabilizes **TS**(S_N2Li-2) more than the other TSs obtained. While the barrier for **TS**(Ad_N–E) turned out to be as large as 51.1(57.0) kcal mol^{-1}, that of **TS**(S_N2Li-2) is very low, as low as 4.1(7.6) kcal mol^{-1}.

The activation energy of the S_N1-like mechanism was calculated to be 48.1(63.2) kcal mol^{-1}. Although the activation energy of **TS**(S_N2Li-1) is not as high as those for **TS**(S_N1Li) and **TS**(Ad_N–E), the values is still as large as 34.3(44.2) kcal mol^{-1}. The relative stability of the TSs in THF is in the order **TS**(S_N2Li-2) >> **TS**(S_N2Li-1) > **TS**(S_N1Li), **TS**(Ad_N-E). It is, therefore, concluded that the reaction of Eq. 1 proceeds under the S_N2-type mechanism through **TS**(S_N2Li-2) in THF.

CONCLUDING REMARKS

The substitution reaction on the vinylic carbon of Eq. 1 has three candidates of mechanisms, the Ad_N–E, the S_N1-like and the S_N2-type mechanisms. The present *ab inito* MO calculations proved that there existed all the reaction paths depending on the position of the counter cation Li^+. The calculations in the gas phase could not determine which is the route applicable to the reaction of Eq. 1 since the calculated activation energies are 30–40 (35-55) kcal mol^{-1} at the B3LYP/6-31+G*//RHF6-31+G* (MP2/6-31+G**//RHF/6-31+G*) level of theory. These values are larger than that expected from the experiments. The calculations including the solvent effect within the SCRF-IPCM model distinguished the route with the lowest activation energy, that is, the S_N2-type mechanism with **TS**(S_N2Li-2) which has Li^+ between the F of the CF_2 fragment and the mesyl oxygen.

The present study suggested the possibility that the S_N2-type reaction proceeded through the **TS**(S_N2Li-1), in which the terminal CF_2 fragment is not directly involved in the reaction. This result explains inverted products obtained by Brown *et al.*[6] In their reaction of (1-bromo-1-alkenyl)boronic esters and organolithiums, Li^+ can locate between B and a leaving group Br in the anionic intermediate such as **6b**. Unlikely to the methyl groups in **6b** the boronic ester fragment used does not disturb the interaction between Li^+ and solvents. Oxygen atoms in the ester fragment also release electrostatic stabilization with Li^+. Therefore, a facile S_N2-type reaction proceeded setereoselectively.

ACKNOWLEDGMENT

The authors thank to the Computer Center, Institute for Molecular Science at the Okazaki National Research Institutes for the use of the NEC HSP computer and the Library Program GAUSSIAN94. This

work was supported by the Grant-in-Aid for Scientific Research (No. 11650847) form the Ministry of Education, Sports and Culture, Japan.

REFERENCES AND NOTES

1. Ichikawa, J.; Sonoda, T.; Kobayashi, H. *Tetrahedron Lett.* **1989**, 30, 1641.

2. (a) Ichikawa, J. *J. Syn. Org. Chem. Jpn.* **1996**, 54, 654. (b) Ichikawa, J.; Fujiwara, M.; Nawata, H.; Okauchi, T.; Minami, T. *Tetrahedron Lett.* **1996**, 37, 8799 and references therein.

3. Chambers, R. D.; James, S. R. *Comprehensive Organic Chemistry*; Stoddart, J. F. Ed.; Pergamon Press: Oxford, **1979**; Vol. 1, pp. 545-547.

4. Hori, K.; Fukuda, S.; Kawano, Y.; Ichikawa, J. *JCPE Journal*, **1999**, 11, 23.

5. (a) Rappoport, Z. *Adv. Phys. Org. Chem.* **1969**, 7,1. (b) Modena, G. *Acc. Chem. Res.* **1971**, 4, 73. (c) Rappoport, Z. *Acc. Chem. Res.* **1981**, 14, 7. (d) Rappoport, Z. *Acc. Chem. Res.* **1992**, 25, 474.

6. Brown H, C.; Bhat, N. G.; Iyer, R. *Tetrahedron. Lett.*, **1991**, 32, 3655.

7. (a) Ochiai, M.; Oshima, K.; Masaki, Y. *J. Am. Chem. Soc.* **1991**, 113, 7059. (c) Okuyama, T.; Ochiai, M. *J. Am. Chem. Soc.* **1997**, 119, 4785.

8. (a) Lucchini, V.; Modena, G.; Pasquato, L. *J. Am. Chem. Soc.* **1993**, 115, 4527. (b) Glukhovtsev, M. N.; Pross, A.; Radom, L. *J. Am. Chem. Soc.* **1994**, 116, 5961. (b) Lucchini, V.; Modena, G.; Pasquato, L. *J. Am. Chem. Soc.* **1995**, 117, 2297.

9. Midland, M. M. *J. Org. Chem.*, **1998**, 63, 914.

10. Frisch, M. J.; Trucks, G. W.; Schlegel, H. B.; Gill, P. M. W.; Johnson, B. G.; Robb, M. A.; Cheeseman, J. R.; Keith, T.; Petersson, G. A.; Montgomery, J. A.; Raghavachari, K.; Al-Laham, M. A.; Zakrzewski, V. G.; Ortiz, J. V.; Foresman, J. B.; Cioslowski, J.; Stefanov, B. B. ; Nanayakkara, A.; Challacombe, M.; Peng, C. Y.; Ayala, P. Y.; Chen, W.; Wong, M. W.; Andres, J. L.; Replogle, E. S.; Gomperts, R.; Martin, R. L.; Fox, D. J.; Binkley, J. S.; Defrees, D. J.; Baker, J.; Stewart, J. P.; Head-Gordon, M.; Gonzalez, C.; Pople, J. A. Gaussian, Inc., Pittsburgh PA, **1995**.

11. (a) K. Fukui, *Acc. Chem. Res.*, **1981**, 14, 363. (b) M. Head-Gordon, J. A. Pople, *J. Chem. Phys.* **1988**, 89, 5777.

12. (a) Lee, C.; Yang, W.; Parr, R.G. *Phys. Rev.* **1988**, *B* 37, 785. (b) Miehlich B.; Savin, A.; Stoll, H.; Preuss, H. *Chem. Phys. Lett.* **1989**, 157, 200. (c) Becke, A.D. *J. Chem. Phys.* **1993**, 98, 5648.

13. Total energies of **3b** and the TS for the S_N1-like mechanism were calculated to be (–1084.26087) and –1079.7233 (-1084.19116) Hartree at the RHF/6-31+G* (B3LYP/6-31+G*//RHF/6-31+G*) level of theory.

14. (a) Foresman, J. B.; Keith, T. A.; Wiberg, K. B.; Snoonian, J.; Frisch, M. J. *J. Phys. Chem.* **1996**, 100, 16098. (b) We used the dielectric constant of THF (5.9) for the SCRF calculations.

15. The SCF convergence of the IPCM calculations for **8b** and **TS**(S_N1Li) were not so good so that the energies include error of ±0.75 and ±0.04 kcal mol ^{1}, respectively. These small errors does not reflect to the discussions in the present study.